doi:10.1017/S1431927622002756
Microsc. Microanal. 28 (Suppl 1), 2022

Mapping of Space Weathering Features and Vesicle Contents in Lunar Soils

K.D. Burgess[1*], B.A. Cymes[2], R.M. Stroud[1]

[1] U.S. Naval Research Laboratory
[2] NRC Postdoctoral Fellow, U.S. Naval Research Laboratory
* Corresponding author: kate.burgess@nrl.navy.mil

The alteration of the surfaces of airless bodies such as the Moon due to interactions with the space environment is known as space weathering. The dominant space weathering processes on the Moon are charged particle irradiation and micrometeorite bombardment. These affect the top few hundred nanometers of individual rocks and dust grains, referred to as a space weathered rim. Our current research utilizes scanning transmission electron microscopy (STEM) imaging, electron energy loss spectroscopy (EELS) and energy dispersive spectroscopy (EDS) to better differentiate the effects of the dominant space weathering processes and understand the ways that these processes alter individual mineral and glass phases.

Irradiation by the solar wind leads to structural and chemical alteration and often amorphization of the very surface of exposed materials [1]. In iron-bearing phases such as olivine, pyroxene, and ilmenite, this can lead to the formation in the rim of small inclusions of metallic iron known as nanophase Fe or $npFe^0$ [2,3]. Hydrogen and helium, the most abundant ions in the solar wind, can be trapped within the irradiated rim, potentially forming vesicles the contents of which can be analyzed using EELS in the STEM [2,4]. At the same time the samples are being irradiated, space-exposed material is being bombarded by micrometeorites, which can cause melting and vaporization [5]. The melt splashes and vapor deposits accumulate in thin layers on neighboring grains and often include $npFe^0$ and vesicles as well.

We prepared samples from several soil grains from lunar sample 79221, a mature high-Ti basalt that has on average experienced significant space weathering. The grains were mounted in epoxy such that one surface of the grain was available for imaging in the scanning electron microscope (SEM). Focused ion beam (FIB) samples were prepared with an FEI Helios G3 equipped with an Oxford 150 mm^2 SDD EDS. We identified several phases, including apatite and Fe metal, that have not been well-studied for their space weathering responses. After imaging, protective carbon straps were deposited on regions of interest, first with e-beam then i-beam. A section suitable for STEM analysis was extracted using standard techniques and mounted on a Cu half-grid. STEM analysis was performed with the Nion UltraSTEM200-X at NRL. The microscope is equipped with a Gatan Enfinium ER spectrometer for EELS and a windowless, 0.7 sr Bruker SDD-EDS detector. Data were collected at 200 kV.

Apatite ($Ca_5(PO_4)_3(F,Cl,OH)$) is present in minor amounts on many Solar System bodies, including the Moon, where it is the most common naturally water-bearing phase [6]. The ability of apatite to contain and retain water in its crystal structure makes it unique among lunar minerals. Its low abundance compared to the main silicate phases means its response to space weathering has not been studied. Additionally, because it is very different in composition from the most common minerals, which are silicates and oxides, any deposition layer is straightforward to separate from a rim formed by irradiation of the substrate grain. Figure 1 shows a region where a vesicular "melt bleb" is present along the surface of the apatite grain with a vesicular rim present in the apatite. The EDS map (Fig. 1b) shows that the bleb is rich in Si and Ti (as well as Fe, Mg, Al) and has variable composition over 10s of nanometers. The apatite composition in the rim surrounding the vesicles is uniform.

EELS low-loss spectrum imaging can be used to gain further information about the vesicles and their content. Figure 1c shows a map of a water signal associated with the vesicles created using a linear least-squares fit of the "bulk" and "difference" spectra shown in Fig. 1d. The "vesicle" spectrum is from a single pixel from the spectrum image. The fitting routine relies on pre-determined end-member spectra, but is able to pick out a number of pixels where the signal due to water trapped in the vesicle is not as obvious. Water and helium, which can also be trapped in space weathering rim vesicles [2,4], are not measureable using only EDS, but can be analyzed using the low-loss region of EELS, as perturbations to the plasmon feature of the weathered phase.

The combination of STEM-EDS maps and EELS data provides a powerful way to interrogate the space weathered surfaces of lunar and other planetary samples and increase our understanding of the processes that alter the surfaces of airless bodies. The physical and chemical alterations take place on the scale of nanometers, but the sum of the changes affect the optical properties of the bodies as a whole, altering how the surfaces look to telescopic and space craft spectrometers. The formation of vesicles and trapping of volatiles, such as the water seen in this apatite grain, could also affect lunar water cycling, exosphere composition, and access to these volatiles for in situ resource utilization (ISRU) [7,8], which will be important for robotic and human exploration of the Moon over the next decade [9].

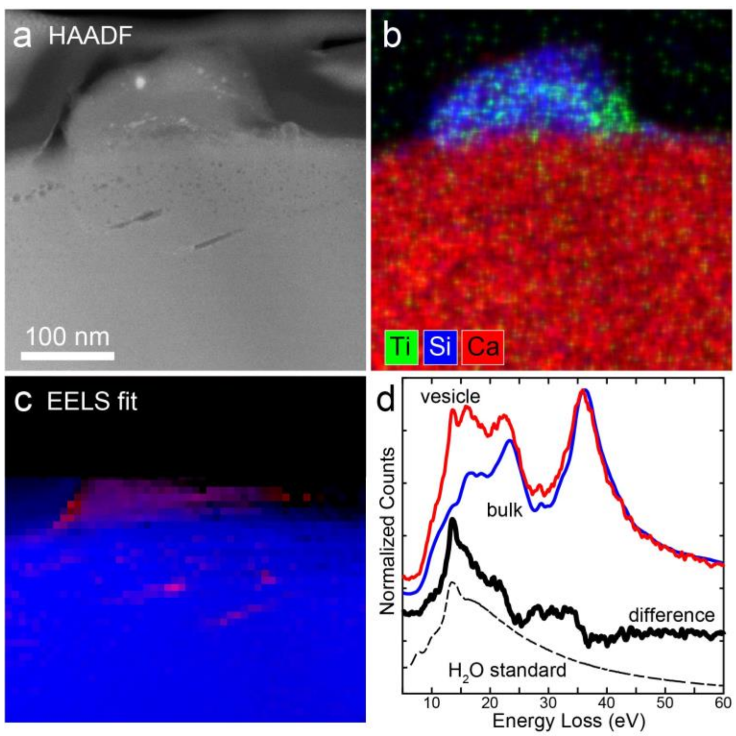

Figure 1. (a) HAADF image showing vesicular space weathered rim in a lunar apatite grain. (b) Semi-quantitative EDS mapping shows that the "melt bleb" on the apatite is rich in Si and Ti and spatially variable. (c) Map of water in the vesicular rim associated with the largest vesicles based on linear least squares fitting of the EELS low-loss spectrum image. (d) Selected spectra from the spectrum image showing the large water signal in a single pixel from within a vesicle compared to the average apatite spectrum. H_2O standard is from [10].

References:

[1] Keller, L.P., and McKay, D.S., Geochim Cosmochim Acta **61** (1997) 2331 10.1016/S0016-7037(97)00085-9.
[2] Burgess, K.D., and Stroud, R.M., Geochim Cosmochim Acta **224** (2018) 64 10.1016/j.gca.2017.12.023.
[3] Burgess, K.D., and Stroud, R.M., Meteor Planet Sci **56** (2021) 10.1111/maps.13692.
[4] Bradley, J.P., et al., Proc Nat Acad Sci **111** (2014) 1732 10.1073/pnas.1320115111.
[5] Pieters, C.M., and Noble, S.K., J Geophys Res **121** (2016) 1865 10.1002/2016JE005128.
[6] Robinson, K.L., and Taylor, G.J., Nat Geosci **7** (2014) 401 10.1038/ngeo2173.
[7] Anand, M., et al., Planet Space Sci **74** (2012) 42 10.1016/j.pss.2012.08.012.
[8] Benna, M., et al., Nat Geosci **12** (2019) 333 10.1038/s41561-019-0345-3.
[9] The authors acknowledge funding from NASA through ANGSA and SSERVI RISE2 programs.
[10] Cassidy, C., et al., PLOS ONE **12** (2017) e0186899 10.1371/journal.pone.0186899.

https://doi.org/10.1017/S1431927622002756 Published online by Cambridge University Press